Detailed study of K_{e4} decay properties by the NA48/2 experiment at CERN

Michal Zamkovsky on behalf of the NA48/2 Collaboration

Institute of Particle and Nuclear Physics, Charles University in Prague, Czech Republic

Abstract

A sample of 1.13 million K_{e4}^{+-} ($K^{\pm} \to \pi^+ \pi^- e^{\pm} \nu$) decays and 65210 K_{e4}^{00} ($K^{\pm} \to \pi^0 \pi^0 e^{\pm} \nu$) decays has been collected in 2003-2004 by the NA48/2 collaboration at the CERN SPS. Branching ratio and form factors in the S- and P-wave have been measured at a percent level precision. The comparison of Branching ratio and form factor values in both modes sheds new light on isospin symmetry breaking effects. Form factor measurements are major inputs to the study of low energy QCD and bring stringent tests of Chiral Perturbation Theory predictions.

Keywords: kaon, form factor, branching ratio, scattering lengths, ChPT

1. The K_{e4} decay formalism

Four-body final state decays are described by five kinematic variables, namely for K_{e4} decays, the Cabibbo-Maksymowicz variables [1]: two invariant masses $S_{\pi} = M_{\pi\pi}^2$ and $S_e = M_{e\nu}^2$ and three angles ϑ_{π}, ϑ_e and φ. The hadronic current is described by form factors which can be developed in a partial wave expansion as suggested in [2]. Limiting the expansion of the decay amplitude to S- and P-waves, two complex axial form factors: $F = F_s \, e^{i\delta_s} + F_p \, e^{i\delta_p} cos\theta_{\pi}$, $G = G_p \, e^{i\delta_{pg}}$ and one complex vector form factor: $H = H_p \, e^{i\delta_{ph}}$ will contribute, where δ_l is the phase of the corresponding $\pi\pi$ scattering amplitude. From the differential rate study in the five-dimensional space, four real form factors and one phase $\delta = \delta_s - \delta_p$, assuming identical phase for the P-waves form factors (F_p, G_p, H_p), are measured, together with their energy variation with S_{π} and S_e. The scattering lengths are extracted from the variation of δ with S_{π} using Roy equations solutions [3] and Isospin breaking mass corrections [4].

In the neutral pion mode K_{e4}^{00}, the variables ϑ_{π} and φ are irrelevant due to Bose statistics. The dipion $\pi^0 \pi^0$ system is only in a S-wave state and the form factors reduce to a single complex form factor: $F = F_s \, e^{i\delta_s}$. The decay amplitude is then proportional to F_s^2 determined in the (S_{π}, S_e) plane.

2. Experimental setup

The primary 400 GeV/c SPS proton beam impinging on a beryllium target produces two simultaneous $K^{\pm}$ beams with a central momentum of (60 ± 3) GeV/c. The secondary beams are focused ~ 200 m downstream at the first spectrometer chamber with a transverse size ~ 10 mm. The decay volume, a 114 m long evacuated vacuum tank, is followed by a magnetic spectrometer (a dipole magnet surrounded by two sets of drift chambers) housed in a tank filled with helium at nearly atmospheric pressure. The momentum resolution achieved in the spectrometer is $\sigma_p/p = (1.02 \oplus 0.044 \cdot p)\%$ (p in GeV/c). The spectrometer is followed by a scintillator hodoscope consisting of two planes segmented into horizontal and vertical strips achieving a very good ~ 150 ps time resolution. A liquid krypton calorimeter (LKr) measures the energy of electrons and photons. The transverse segmentation into 13248 2 cm $\times$ 2 cm projective cells and the 27 radiation length thickness result in an energy resolution $\sigma(E)/E = (3.2/\sqrt{E} \oplus 9.0/E \oplus 0.42)\%$ (E in GeV/c) and a transverse position resolution ~ 1.5 mm for 10 GeV isolated showers. This allows to separate electrons ($E/p \sim 1$) from pions ($E/p < 1$). A hadron calorimeter and muon veto counter are located further downstream. A two-level trigger logic selects and flags events with a high effi-

ciency for both K_{e4} topologies. A detailed description is available in [5].

3. K_{e4} selection and reconstruction

Event reconstruction and selection for the charged K_{e4}^{+-} mode require three tracks reconstructed by the magnetic spectrometer, forming a vertex within the decay volume without any associated hit in the muon veto counters. For the neutral K_{e4}^{00} mode, event reconstruction requires two cluster pairs of photons satisfying the π^0 mass constraint, vertices of neutral pions within decay volume and closer than 500 cm from each other, and CDA (Closest Distance of Approach) of charged track to the beam lime closer than 800 cm from the mean of π^0's vertices. The reconstruction follows the same paths for both signal and more abundant $K_{3\pi}$ ($K^\pm \to \pi^+\pi^-\pi^\pm$ and $K^\pm \to \pi^0\pi^0\pi^\pm$) normalization modes. They are recorded concurrently with the same trigger logic. Kinematic separation of signal and normalization candidates is obtained by requiring (or not) missing mass and missing transverse momentum in the $K_{3\pi}$ hypothesis. Extra requirements of electron identification ($0.9 < E/p < 1.1$ and properties of LKr associated shower consistent with the electron hypothesis) ensure a low background contamination of order $\sim 1\%$ relative to signal. The remaining background is mainly due to $K_{3\pi}$ decays with a $\pi^\pm$ faking an electron response in LKr or followed by the rare $\pi \to e\nu$ decay, while accidental coincidence with another track/photon is one order of magnitude lower. Most background contributions are measured from control data samples. Geometrical acceptances for the four decay modes are obtained from a MC simulation including beam and detector geometry, material description and local detector imperfections.

4. Form factor and scattering lengths measurement

Form factors values are obtained by adjusting the differential distributions of simulated signal candidates to those of data candidates in small boxes of the multidimensional kinematical space. The F_s form factor variations with $q^2(= S_\pi/4m_{\pi^+}^2 - 1)$ are displayed in Fig.1. The same quadratic behavior is present in both modes for ($q^2 > 0$) and a deficit of events is observed below the $2m_{\pi^+}$ threshold ($q^2 = 0$) in the K_{e4}^{00} mode as observed in the $K_{3\pi}^{00}$ mode [6]. It can be explained by final state charge exchange scattering ($\pi^+\pi^- \to \pi^0\pi^0$). The absolute form factors have also been obtained as:

$$F_S(K_{e4}^{+-}) = 5.705 \pm 0.017_{exp} \pm 0.031_{ext} \quad (1)$$
$$F_S(K_{e4}^{00}) = 6.079 \pm 0.030_{exp} \pm 0.046_{ext}.$$

The energy dependence of F_s is described as a polynomial expansion in q^2 (or as a cusp function) and $\dfrac{S_e}{4m_{\pi^+}^2}$:

$$F_s = f_s\left(1 + aq^2 + bq^4 + c\frac{S_e}{4m_{\pi^+}^2}\right) q^2 > 0, \quad (2)$$
$$F_s = f_s\left(1 + d\sqrt{|q^2/(1 + q^2)|} + c\frac{S_e}{4m_{\pi^+}^2}\right) q^2 < 0.$$

The isospin 0 and 2 S-wave scattering lengths a_0^0, a_0^2 for $\pi\pi$ scattering are obtained from the phase measurement:

$$a_0^0 = 0.222 \pm 0.013_{exp} \quad (3)$$
$$a_0^2 = -0.043 \pm 0.009_{exp}.$$

These results can be combined with the independent measurements of the $K_{3\pi}^{00}$ study [6] to more precise values:

$$a_0^0 = 0.221 \pm 0.006_{exp} \quad (4)$$
$$a_0^2 = -0.043 \pm 0.005_{exp}.$$

The fit results from K_{e4}^{+-} and $K_{3\pi}^{00}$ data are shown in Fig. 2 together with the measurement from pionium atom lifetime [7] and theoretical prediction [8, 9].
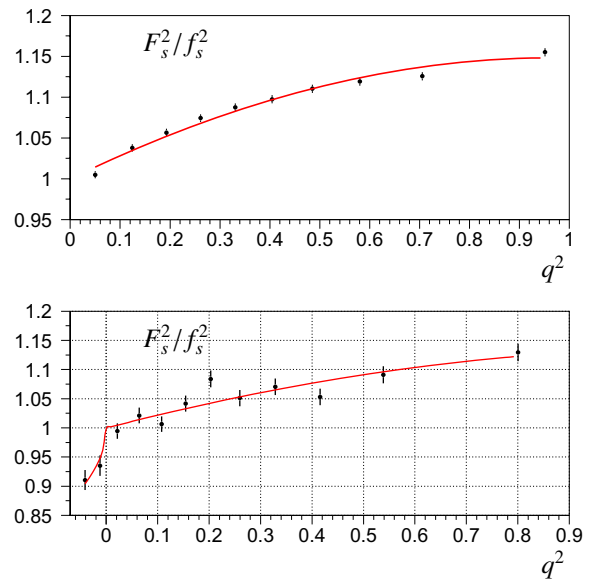

Figure 1: Relative F_s^2/f_s^2 form factor measurements function of q^2 in the K_{e4}^{+-} (**Top**) and the K_{e4}^{00} (**Bottom**) mode. By construction $F_s^2/f_s^2(q^2 = 0) = 1$. Red lines are degree-2 polynomial fits to the data (stat. errors only) for $q^2 > 0$.
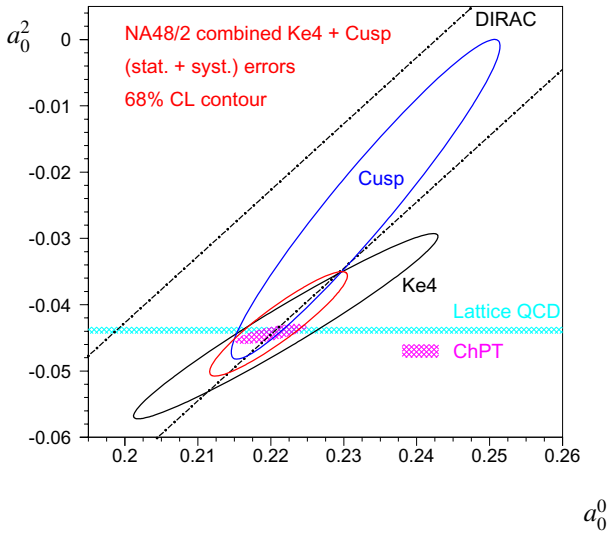
Figure 2: Fits of the NA48/2 K_{e4} data in the (a_0^0, a_0^2) plane.

5. Branching ratio measurement

Branching ratios (BR) are obtained as:

$$\mathrm{BR}\left(K_{e4}\right) = \frac{N_s - N_b}{N_n} \cdot \frac{A_n \varepsilon_n}{A_s \varepsilon_s} \cdot \mathrm{BR}\left(K_{3\pi}\right), \qquad (5)$$

where N_s, N_b, N_n are numbers of signal candidates, background contribution and normalization events, ε_s and ε_n are the trigger efficiencies for signal and normalization, A_s and A_n are the geometrical acceptances and BR ($K_{3\pi}$) is the normalization Branching ratio. The trigger efficiencies are well above 95% and similar for signal and normalization modes. Acceptances are typically $\sim 18 - 20\%$ in the K_{e4}^{+-} and $K_{3\pi}^{+-}$ modes and 2% (4%) in the K_{e4}^{00} ($K_{3\pi}^{00}$) modes. For the charged mode, the world average (2012) precision of 2.4% is improved by a factor of 3, now 0.8%, dominated by the external error (0.7%):

$$\mathrm{BR}\left(K_{e4}^{+-}\right) = (4.257 \pm 0.016_{exp} \pm 0.031_{ext}) \times 10^{-5}. (6)$$

The detailed form factor and BR measurements are available in [10]. For the neutral mode, the world average (2012) precision of 18% is improved by more than one order of magnitude, now 1.4%, dominated by the external error (1.25%):

$$\mathrm{BR}\left(K_{e4}^{00}\right) = (2.552 \pm 0.014_{exp} \pm 0.032_{ext}) \times 10^{-5}. (7)$$

The experimental error combines quadratically statistical and systematic errors, including uncertainties on acceptance, resolution, beam geometry, particle identification, trigger efficiencies and radiative corrections.

External errors stem from the normalization mode BR uncertainties and are the dominant errors. More details on the neutral mode form factor and BR measurements are available in [11].
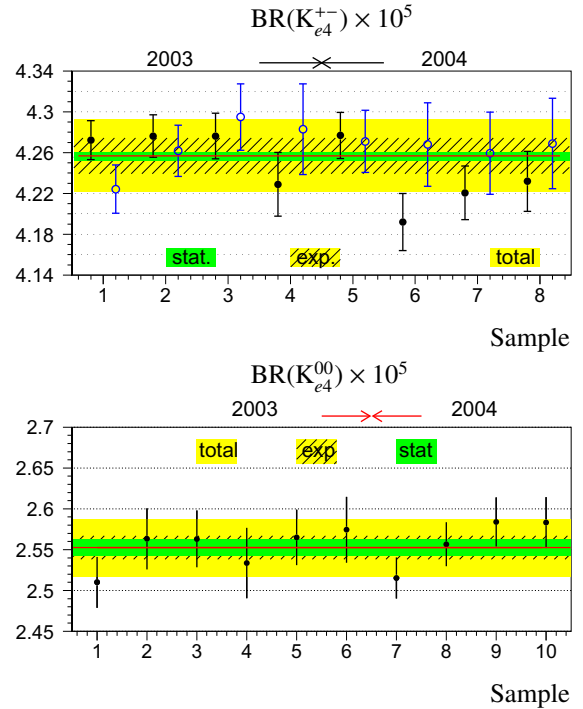

Figure 3: BR(K_{e4}^{+-}) (**Top**, full dots for K^+, open dots for K^-) and BR(K_{e4}^{00}) (**Bottom**, K^+, K^- combined) for statistically independent samples. Each error bar corresponds to the sample-dependent error of statistical origin. The line and the inner band correspond to the result of the weighted average and its statistical error.

References

[1] N. Cabibbo and A. Maksymowicz: *Phys. Rev.* **B438**, (1965) 137.
[2] A. Pais and S. Treiman: *Phys. Rev.* **168**, (1968) 1858.
[3] B. Ananthanarayan, G. Colangelo, J. Gasser, H. Leutwyler: *Phys. Rept.* **353**, (2001) 207.
[4] G. Colangelo, J. Gasser, A. Rusetsky: *Eur. Phys. J.* **C59**, (2009) 777.
[5] V. Fanti *et al*: *Nucl. Instrum. Methods* **A574**, (2007) 433.
[6] J. Batley *et al*: *Eur. Phys. J.* **C64**, (2009) 589.
[7] B. Adeva *et al*: *Phys. Lett.* **B704** (2011) 24.
[8] G. Colangelo, J. Gasser, H. Leutwyler: *Phys. Rev. Lett.* **86** (2001) 5008.
[9] X. Feng, K. Jansen, D. Renner: *Phys. Lett.* **B684** (2010) 268.
[10] J. Batley *et al*: *Eur. Phys. J.* **C70**, (2010) 635, *ibidem*, *Phys. Lett.* B **715**, (2012) 105.
[11] J. Batley *et al*: *JHEP* **08** (2014) 159.